On the propagation of low-frequency fluctuations in the plasma sheet: 2. Characterization of the MHD eigenmodes and physical implications

G. Fruit, P. Louarn, E. Budnik, J.A. Sauvaud, C. Jacquey, D. Le Quéau, H. Rème, E. Lucek, A. Balogh, N. Cornilleau-Wehrlin

On the propagation of low-frequency fluctuations in the plasma sheet: 2. Characterization of the MHD eigenmodes and physical implications

G. Fruit,[1] P. Louarn,[2] E. Budnik,[2] J. A. Sauvaud,[2] C. Jacquey,[2] D. Le Quéau,[2] H. Rème,[2] E. Lucek,[3] A. Balogh,[3] and N. Cornilleau-Wehrlin[4]

Received 9 September 2003; revised 22 December 2003; accepted 23 January 2004; published 24 March 2004.

[1] In a first analysis of the low-frequency fluctuations observed by Cluster during a crossing of the plasma sheet [*Louarn et al.*, 2004], we identify oscillations that likely correspond to MHD eigenmodes. They are intense (10 nT), have a rather short period (20–25 s), have a wavelength of $\sim$5 R_e, and are observed during an active period that follows a substorm onset. We show here that they combine both sausage and kink modes propagating in the x direction with a common spectral peak at $\sim$0.04 Hz, the sausage oscillations presenting also a secondary peak at 0.13 Hz. Using a complete theory of the linear MHD response of the plasma sheet, we reconstruct the sheet oscillations starting from given external perturbations. This method leads to quantitative predictions concerning the magnetic and pressure fluctuations. The existence of natural resonant frequencies of the sheet can indeed be foreseen and the relative weight of the kink-like and sausage-like modes can also be estimated. We show that the kink mode (0.04 Hz) and the high-frequency sausage mode (0.14 Hz) are perfectly compatible with the MHD model of Harris sheet oscillations, with wavelength of $\sim$6 R_e and $\sim$3 R_e, respectively. The corresponding amplitude of the pressure and magnetic fluctuations also appears to be remarkably consistent with the theoretical predictions. Conversely, the low-frequency sausage mode (0.04 Hz) is hardly explained by the MHD model. We propose that it could be a nonideal MHD or a kinetic mode, as the tearing mode. *INDEX TERMS:* 2744 Magnetospheric Physics: Magnetotail; 2752 Magnetospheric Physics: MHD waves and instabilities; 2764 Magnetospheric Physics: Plasma sheet; 2788 Magnetospheric Physics: Storms and substorms; *KEYWORDS:* magnetotail, MHD waves and instabilities, plasma sheet, storms and substorms

Citation: Fruit, G., P. Louarn, E. Budnik, J. A. Sauvaud, C. Jacquey, D. Le Quéau, H. Rème, E. Lucek, A. Balogh, and N. Cornilleau-Wehrlin (2004), On the propagation of low-frequency fluctuations in the plasma sheet: 2. Characterization of the MHD eigenmodes and physical implications, *J. Geophys. Res.*, *109*, A03217, doi:10.1029/2003JA010229.

1. Introduction

[2] In a first paper [*Louarn et al.*, 2004, hereinafter referred to as paper 1], we apply the theory of the MHD propagation in a Harris sheet to interpret the low-frequency oscillations observed by Cluster during a crossing of the sheet. This study is based on the analysis of the spatial/temporal scales of the fluctuations. The MHD theory indeed predicts that the periods of the eigenmodes of the sheet are scaled by a characteristic time (τ) equal to the ratio between (1) the thickness of the sheet and (2) the sound speed. Using the four Cluster spacecraft, the sheet thickness and thus τ can be precisely estimated. By comparing this characteristic time with the timescale of the fluctuations, it is possible to estimate their wavelength, assuming that they are MHD-type oscillations. Since freely propagating eigenmodes observable by Cluster cannot have a wavelength larger than typically 15 R_e, the distance between Cluster and the inner magnetosphere, we classify the fluctuations and identify those that could correspond to MHD eigenmodes. During the crossing on 22 August 2001, we show that fluctuations with periods larger than 100–150 s cannot be freely propagating MHD eigenmodes. Conversely, fluctuations with periods of 20–25 s appear to be good candidates for MHD eigenmodes. They could indeed be kink-like waves propagating in the x direction with wavelength of the order or smaller than 5–7 R_e.

[3] Having identified these possible MHD fluctuations, we perform here a more precise analysis. As shown by *Fruit et al.* [2002], the theory of the MHD propagation in a Harris sheet remains sufficiently simple to allow a complete analysis of the linear response of the plasma sheet. The exact structure of the eigenmodes can be computed. It is

[1]Department of Mathematics, University of Waikato, Hamilton, New Zealand.
[2]Centre d'Etude Spatiale des Rayonnements, Toulouse, France.
[3]Imperial College, London, UK.
[4]Centre d'Etudes Terrestres et Planétaires, Vélizy, France.

0148-0227/04/2003JA010229

also possible to consider various types of external excitations, for example by considering initial pressure pulses or displacements of the sheet, and to compute their coupling with the MHD eigenmodes. The complete spatiotemporal evolution of the sheet can then be reconstructed by an inverse Fourier-Laplace transform of the linear combination of the eigenmodes. For a given initial excitation, this complete analysis of the linear response of the system leads to quantitative estimates of the amplitude of both the pressure and the magnetic perturbations. It also predicts the possible existence of preferred frequencies in the response of the sheet and the relative importance of kink-like and sausage-like oscillations. We stress again that our theoretical analysis is restricted to a propagation in the x direction. As discussed later, this hypothesis is supported by the observations. A detailed reference list concerning the low-frequency propagation in the plasma sheet may be found in paper 1. We do not remind it here.

[4] In section 2 we identify the different modes that propagate in the sheet and show that both sausage and kink modes are detected. The comparison with the theory is performed in section 3, where we present a reconstruction of the oscillations and determine both their spectral features and amplitudes. We show that the kink mode (0.04 Hz) and the higher-frequency sausage mode (0.14 Hz) agree very well with the MHD theory. This is not the case of the low-frequency sausage mode (0.04 Hz) and alternative explanations have to be proposed. This mode could be a tearing mode and be related to nonideal or kinetic effects.

2. Analysis of Plasma Sheet MHD-Like Oscillations

2.1. Observations

[5] Following the analysis proposed in paper 1, we consider the time period 0948–0957 UT, 22 August 2001, during which possible MHD eigenmodes have been observed. The corresponding CIS (ion spectrometer) and FGM (magnetometer) Cluster data are displayed in Figure 1. Starting from the top of the figure, the magnetic X, Y, Z components (panels 1, 2, and 3), the density (panel 4), the temperature (panel 5), the thermal pressure (panel 6), the total pressure (magnetic + thermal) (panel 7), and the velocity X component (panel 8) are shown. The usual color code is used: measurements performed by SC1, 2, 3, 4 are in black, red, green, and blue, respectively. We consider here data from the CODIF-CIS instrument. This instrument is not operational on SC2, hence the lack of corresponding ion data. The time resolution is 0.2 s for the magnetic field and 4 s for the plasma measurements. Below, the respective positions of the spacecraft are indicated in the GSM frame.

[6] The general context of this observations has been discussed in paper 1. To summarize, Cluster is in the lobe before 0942 UT and enters the plasma sheet from 0942 to 0943 UT (see Figure 3, paper 1). A high-velocity earthward flow is simultaneously observed and, as suggested by ground measurements, the magnetosphere is becoming more active. The time period considered in Figure 1 thus follows the propagation of large-scale perturbations in the sheet that are likely associated to a substorm onset. At 0950 UT, the Z magnetic component turns southward and a fast tailward flow is detected for $\sim$10 s. The MHD-like oscillations follow this perturbation and are observed until $\sim$1000 UT. The period shown here corresponds to the most intense fluctuations. Comparing the four spacecraft measurements, one notices that the current sheet thins after 0950 UT. As discussed in paper 1, the sheet thickness becomes as small as $\sim 0.2-0.3\ R_e$ from 0950 to 0954. In this time range the temperature is about 4 keV leading to a sound speed $\sim$800 km/s. It is a slightly lower value than the one chosen in paper 1 where five hours of data (0700–1200) were considered. The characteristic MHD time τ is short ($\tau \sim 1.5-2$ s) which leads us to conclude that the 20–25 s period oscillations are compatible with MHD kink eigenmodes.

[7] A more detailed examination of Figure 1 shows that the characteristics of the oscillations as well as the structure of the sheet change in time. Two phases can be considered. From 0951 to 0954 UT, SC1, 2, and 4 observe large and regular oscillations of the X magnetic component. Their maximum amplitude reaches 15 nT. These three spacecraft are clearly located inside the current sheet. They observe Y and Z magnetic perturbations that are not so well organized and remain smaller than 5 nT. These fluctuations are thus compressional which is compatible with the polarization of the kink-like or the sausage-like MHD eigenmodes. Meanwhile, SC3, which is located below the three other spacecraft and thus further from the central sheet, does not detect so large X fluctuations. It rather observes large Y fluctuations thus torsional, possibly of the Alfven-type. During this first time period (0951–0954), one also notes that (1) B_z is almost null in average, (2) the different spacecraft, located at different altitudes in the sheet, measure similar total pressure, and (3) the flow velocity remains small (less than 200 km/s). These conditions are perfectly compatible with the use of the Harris sheet model and the doppler shift associated with the flow can be considered as negligible.

[8] The situation changes after 0954 UT. An earthward flow appears. It increases up to 800 km/s at 0956 UT with, simultaneously, an evolution of the nature of the oscillations. They are less regular, their polarity changes since they get large Y and Z components (up to 15 nT). Some large peaks in B_z are also observed. The total pressure measured by SC3 becomes significantly smaller than the one measured by SC1 and SC4, suggesting that the conditions of the equilibrium could have been modified. One indication of the evolution of the equilibrium is the sudden positive shift of the X magnetic components observed by the four spacecraft at 0954. Its simplest explanation is a downward motion of the whole sheet. This time period appears to be less adapted to the use of the simple Harris model. We will thus concentrate our

Figure 1. CIS and FGM observations performed by Cluster from 0948 to 0956 UT, 22 August 2001. Panel 1, 2, 3: magnetic field components; Panel 4: density; Panel 5: temperature; Panel 6: thermal pressure; Panel 7: total pressure; Panel 8: fluid velocity. Below: Cluster positions in GSM frame.

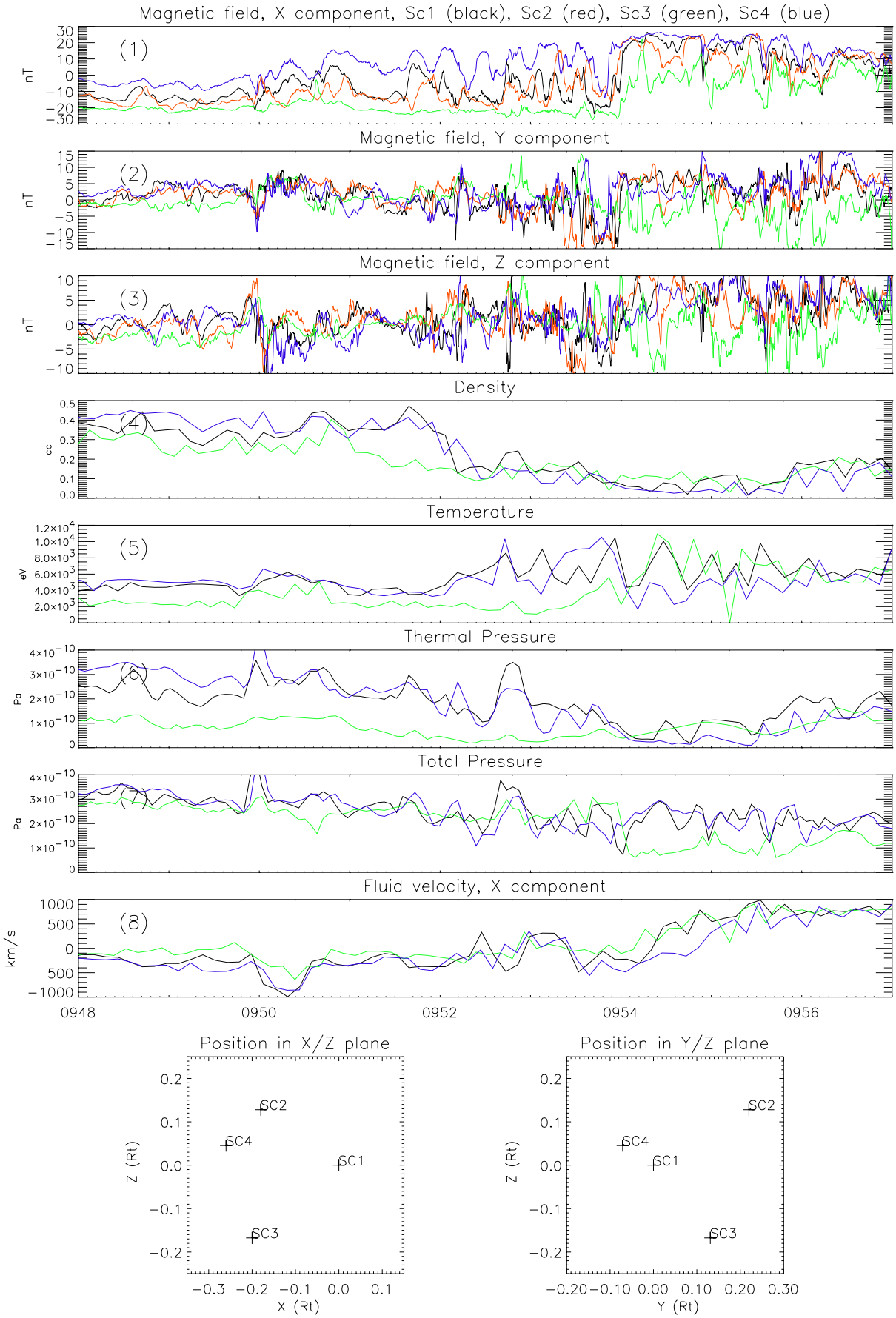
Magnetic field, X component, Sc1 (black), Sc2 (red), Sc3 (green), Sc4 (blue)
(1)
nT
Magnetic field, Y component
(2)
nT
Magnetic field, Z component
(3)
nT
Density
(4)
cc
Temperature
(5)
eV
Thermal Pressure
(6)
Pa
Total Pressure
(7)
Pa
Fluid velocity, X component
(8)
km/s
0948
0950
0952
0954
0956
Position in X/Z plane
SC2
SC4
SC1
SC3
Z (Rt)
X (Rt)
Position in Y/Z plane
SC2
SC4
SC1
SC3
Z (Rt)
Y (Rt)

Figure 1.

analysis to the interpretation of the oscillations observed from 0951 to 0954 UT.

2.2. Structure and Dynamics of the Plasma Sheet

[9] To analyze the spatial-temporal evolution of the sheet, we determine its geometrical parameters from a fit with a Harris sheet. We use here a method comparable to the one developed by *Nakamura et al.* [2002]. The magnetic field is thus supposed to write

$$B_x(z') = B_0 \tanh\left(\frac{z' - z_0}{a}\right), \quad (1)$$

where B_0 is the field in the lobe. Considering that the magnetic pressure in the lobe is equal to the total pressure in the sheet, one obtains $B_0 \sim 25$ nT for the period considered here.

[10] The fitting procedure includes the following stages. First, to insure simultaneity, we resample all measurements to the times of data acquisition of a particular spacecraft chosen as reference (SC1 here). Assuming that the sheet is a monodimensional structure, we determine the normal to the sheet with a simple linear procedure (see paper 1). For the period considered here, the averaged direction of the normal is computed. The thickness and the position of the sheet are then estimated relatively to this direction. The spacecraft positions are thus projected along this axis before applying the fitting procedure. Different sets of spacecraft can then be used to obtain a fit of the measurements with the test function. The reliability of the fit can be controlled by comparing the results [see also *Nakamura et al.*, 2002].

[11] The results are displayed in Figure 2. The panels are numbered from the top of the figure. In panel 1, we present the neutral sheet position z_0 relatively to SC1 (in blue) and the sheet thickness a (in red). For the time period considered here, the average normal to the sheet is (−.24, −.62, .65) in the GSM frame. This indicates that the sheet is tilted by almost 45° in the *Y*/*Z* frame. The tilt significantly modifies the spacecraft positions relatively to the natural frame (*L*, *M*, *N*) of the sheet (*N*: normal to the sheet, *L*: direction of the main field). As seen in Figure 1, for a positive 45° tilt in the *Y*/*Z* plane, SC3 and SC4 are indeed the most distant spacecraft along the direction of the normal, SC1 and SC2 being in between at almost the same altitude but at different *L* and *M* positions. The half-thickness (a) is ∼0.4 R_e until 0950:30 UT. It then decreases to 0.2 R_e from 0951 to 0955:30 UT before increasing gradually again. The short largest fluctuations are likely artificial and may indicate that the sheet loses its 1-D geometry for a short time period. For example, the large fluctuation at 0950:30 is observed during a B_z reversal, thus when the Harris sheet is likely a poor approximation. The quality of the fit can be appreciated by considering different sets of spacecraft. We use (SC1, SC3, SC4) and (SC2, SC3, SC4) and get comparable results which gives confidence on the identification of the nature of the sheet oscillations. These oscillations are particularly regular from 0951:30 to 0954 and concern both the position and the thickness of the sheet which is indicative of the existence of simultaneous kink and sausage modes. As seen in panels 2 and 3, where the projections of the normal to the sheet in the plane *X*/*Z* and *Y*/*Z* (after correction from the averaged tilt) are displayed, the oscillations also correspond to regular variations of the direction of the normal. They are particularly large (up to 30°) and well organized in the *X*/*Z* plane for the period 0952–0954. These large oscillations in the *X*/*Z* plane are consistent with what is expected for a kink mode propagating in the x direction and corresponds to a serpentine-like propagation.

[12] In panel 4 we reconstruct the sheet configuration to get a visual impression of its dynamics. The spacecraft are considered as fixed points, their positions along the normal to the sheet being indicated on the plot (SC1, SC3, and SC4). Using the sheet position (z_0) and thickness (a), we plot its boundaries defined by $z_0 + a$ and $z_0 - a$. This plot presents the sheet undulations with respect to the spacecraft as a function of time. However, if these undulations are MHD eigenmodes, their phase and group velocities would then be of the order of the sound speed (∼800 km/s). This plot would thus also represent the spatial structure of the sheet. We superpose three color bands that indicate the pressure measured by SC1, SC3, and SC4. Their positions in the plot correspond to the actual position of the spacecraft. The detailed analysis of the pressure fluctuations will be performed in section 3.4. One can nevertheless notice some general behaviors. The thinning of the sheet, from 0951:30 to 0954, is associated with a decrease of the thermal pressure (a factor of 2 in average compared with the period 0948–0951). One also notice that the downward motion at 0954 corresponds to a strong pressure unbalance between the upper (SC1 and SC4) and the lower (SC3) spacecraft. This motion would thus be simply interpreted as a reaction of the sheet to modifications in the external pressure conditions.

[13] This presentation of the sheet suggests that the magnetic fluctuations combines both kink and sausage modes. They have an amplitude of the order of 0.1 R_e each and present a particular phasing which explains the observed nonsymmetry between the two side of the neutral sheet. The sheet indeed tends to widen when it moves upward. Hence its upper side presents much larger undulations than the lower one. In the upper side the kink and sausage modes indeed add so that the amplitude of the undulations reaches 0.2 R_e. This is interesting to compare the angular oscillations of the normal with the spatial undulations of the sheet. They have been obtained in two different ways (linear expansion of the field and fit with a Harris sheet, respectively) and the parameter that allows for their comparison is the wavelength of the oscillation. In the present case, assuming that the oscillations are sinusoidal, one can check that angular oscillations of ∼20–30° are compatible with 0.2 R_e undulations if the wavelength is of the order of 7 R_e. The fact that the angular oscillations are more pronounced and well defined in the *X*/*Z* plane means also that the waves mainly propagate is the x direction. Given the wavelength of the oscillations and the interspacecraft distances, the direct determination of the direction of propagation and the wavelength would be here almost impossible by traditional correlation methods. As shown later, wavelengths of the order of 7 R_e are compatible with the theoretical model.

2.3. Identification of Eigenmodes

[14] To have a high-frequency complementary view of the sheet dynamics, we also consider the magnetic fluctuations observed by the STAFF search-coil antenna (see *Cornilleau-Wehrlin et al.* [1997] for details on the STAFF experiment) from 0952 to 0954 UT with a sampling rate of

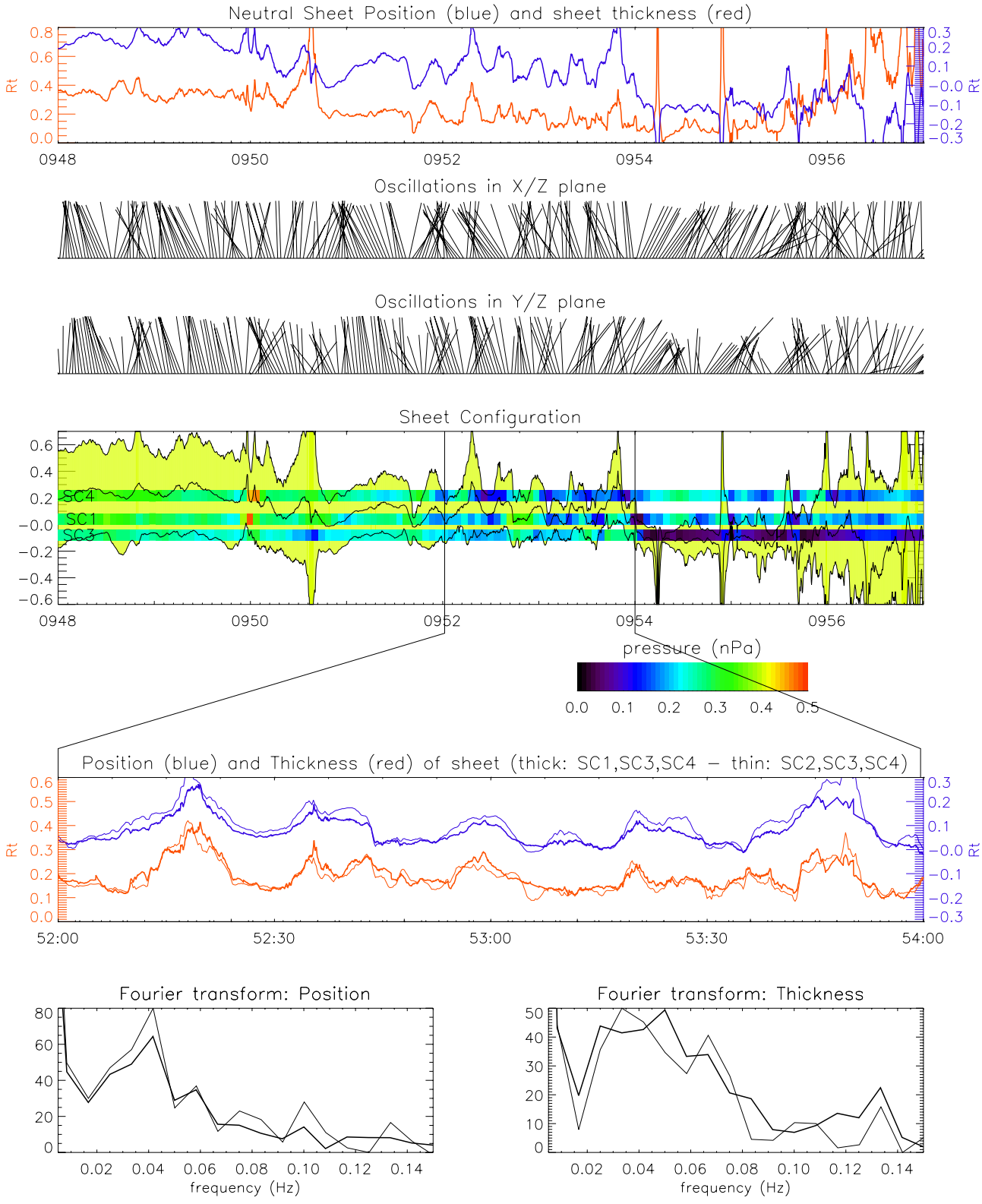

Figure 2. Detailed analysis of the sheet structure. From top panel: (1) neutral sheet position and thickness obtained by a fit with a Harris model; (2) and (3): projections of the normal to the sheet in the *X*/*Z* and *Y*/*Z* plane; (4) sheet configuration and pressure fluctuations measured by spacecraft 1, 3, and 4. (5) and (6): oscillations deduced from STAFF measurements and spectral analysis of thickness and position.

25 p/s. The position and thickness of the sheet determined from these data are presented in thin lines on panel 5, Figure 2. In thick line we present the same parameters estimated from FGM data. In the two plots below, the Fourier transforms of the position and of the thickness are shown, on the left and the right, respectively. We again use both determinations (from FGM and STAFF).

[15] One notices the very good similarity of the two determinations. The neutral sheet undulates between SC1 and SC4 with a typical 20–25 s period. This corresponds to the spectral peak at 0.04 Hz seen in the spectrum of the sheet position. We do not identify a higher frequency peak on this spectrum. The sheet thickness fluctuates in remarkable phase with the position which corresponds to the broad peak centered at 0.04 Hz. Nevertheless, the spectrum also presents a peak at 0.13–0.14 Hz. These results suggest that two sausage-like oscillations, at 0.04 and 0.13 Hz, propagate in the sheet whereas only one kink-like oscillation, at 0.04 Hz, is observed.

[16] The perfect phasing between the position and thickness variations at 0.04 Hz may appear as puzzling. As discussed later, MHD sausage oscillations of the Harris sheet at that frequency are unexpected given the sheet characteristics. Before considering other theoretical models, we examined if this results could be an artifact of the fitting method. Indeed, if the actual sheet is not exactly a Harris sheet, the fitting method will almost systematically give position and thickness varying in phase. We thus considered different models corresponding to various profiles of the sheet. For example, we use magnetic field variations of the form $B(z) = B_0[\tanh((z - z_0)/a)]^n$, corresponding to more or less square-shaped profiles. This does not change the results, and a sausage mode at 0.04 Hz is always detected with even a larger amplitude than presented here. A more radical solution was also tried; we determine the sheet oscillations assuming that its thickness is constant and thus that the sausage mode is absent. The variations of the thickness obtained with the simple Harris fit procedure are then interpreted as variations of the interspacecraft distances when projected along the normal to the sheet. If couples of spacecrafts are used (for example, SC1 and SC4), this method gives acceptable results if couples of spacecraft only are used but leads to inconsistency if more than two spacecraft are considered. Despite theoretical difficulties that are now detailed, we thus conclude that the 0.04 Hz sausage mode actually exists and is not an artifact of the fitting procedure.

3. Comparison With the MHD Theory

3.1. Response of a Harris Current Sheet to an Initial Displacement

[17] To interpret the low-frequency oscillations analyzed in the previous section, we use the theoretical model developed by *Fruit et al.* [2002] that describes the linear response of a Harris sheet to an external perturbation. After time-Laplace and space-Fourier transforms of the MHD equations, the basic equation of the problem writes

$$\frac{d}{dz}\left[f_{\omega,k}(z)\frac{d\hat{\xi}_z}{dz}\right] + g_{\omega,k}(z)\hat{\xi}_z = S_{\omega,k}(z) \tag{2}$$

with

$$f_{\omega,k} = \rho_{eq}\left(v_s^2 + v_A^2\right)\frac{\omega^2 - k^2 v_c^2}{\omega^2 - k^2 v_s^2}, \tag{3a}$$

$$g_{\omega,k} = \rho_{eq}\left(\omega^2 - k^2 v_A^2\right). \tag{3b}$$

[18] We consider here a pure parallel propagation (along x). The second term of equation (2) is the source term related to the excitation. In these equations the prime notation denotes the derivative with respect to z, the different quantities v_s, v_A and v_c are the sound, Alfven, and cusp speeds, respectively. The cusp speed is given by

$$v_c^2 = \frac{v_A^2 v_s^2}{v_A^2 + v_s^2}.$$

[19] The resolution of this equation with boundary conditions corresponding to solutions embedded in the sheet (the transverse displacement vanishes at infinity) yields to discrete eigenmodes in a particular domain of frequencies [see *Fruit et al.*, 2002; *Louarn et al.*, 2004]. Let us note ω_n and $\psi_n(z)$ as the eigenfrequencies and the eigenfunctions. The Green function that corresponds to a unit source term placed at a point z' and oscillating at ω, k can be developed upon the discrete series of eigenfunctions (see equation (19) in the work of *Fruit et al.* [2002]):

$$G_{\omega,k}(z|z') = \sum_{n=0}^{+\infty} \frac{\psi_n(z)\psi_n(z')}{\omega^2 - \omega_n^2}. \tag{4}$$

This equation shows that the eigenfrequencies ω_n are poles for the Green function considered as a function of the complex variable ω. Hence the solution of equation (2) with a given source term reads

$$\hat{\xi}_z(\omega, k, z) = \int_{-\infty}^{+\infty} dz'\ G_{\omega,k}(z|z')S_{\omega,k}(z'). \tag{5}$$

The reconstruction of the spatial temporal perturbations is then made by inverting the Laplace and Fourier transforms. More precisely the inversion of the Laplace transform needs an integration along a contour in the complex ω-plane that runs above all the poles of the Green function (see details in the work of *Fruit et al.* [2002]). The final result can be formally written as

$$\xi_z(t,x,z) = -\frac{i}{2\pi}\sum_{n=0}^{\infty}\int_{-\infty}^{+\infty} dk\, e^{ikx}\,\frac{\psi_n(z)\psi_n(z')}{2\omega_n} \times \left[S_{\omega_n,k}\, e^{-i\omega_n t} - S_{-\omega_n,k}\, e^{i\omega_n t}\right]. \tag{6}$$

[20] *Fruit et al.* [2002] considered an external thermal pressure pulse as the source term. An external current disruption or a perturbation in the static magnetic field could have been chosen as well. One of their important conclusions was to show that such an external excitation yields to very small amplitude oscillations of the plasma sheet. Even by choosing optimal geometries for the pulse, the amplitude of the fluctuations reaches barely a few percents of the initial pulse. Clearly, the amplitude of the oscillations observed by Cluster and presented here is much

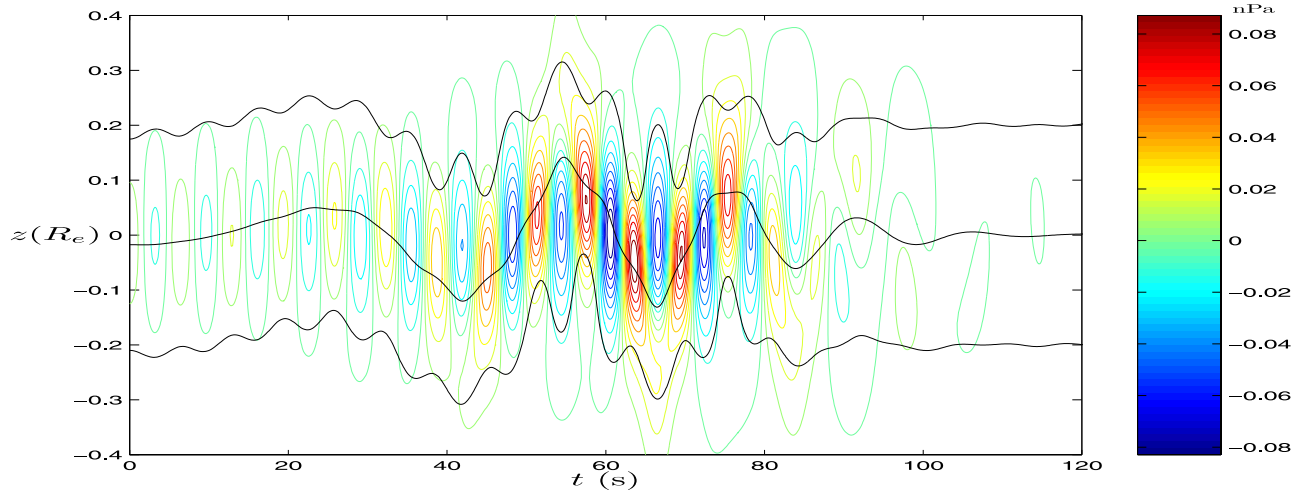

Figure 3. Temporal evolution of the current sheet responding to an initial displacement located at $50a = 10\ R_e$. The three black lines correspond to a constant B_x component and the colored isocontours represent the thermal pressure fluctuations.

too intense to be initiated by such an excitation. We thus consider here other types of initial condition. We suppose that the sheet initially experiences (at $t = 0$) a finite transversal displacement $\xi_z^o(x, z) = \xi_z(t = 0, x, z)$ and then relaxes. The panel 4 of Figure 2 shows that such displacements may exist (see the large displacement at 0954). It is beyond the scope of this paper to discuss the origin of such an initial displacement. Let us nevertheless notice that it could be due to a pressure unbalance between the two sides of the sheet as seen from 0954 to 0956.

[21] This initial condition appears in the above equations through the Laplace transform and the source term reads

$$S_{\omega,k}(z) = i\omega\rho_{eq}(z)\hat{\xi}_z^o(k, z). \tag{7}$$

For practical reasons, we choose an initial displacement gaussian both in x and z directions

$$\xi_z^o(x, z) = Z_0 e^{-x^2/2L_x^2} e^{-(z-z_0)^2/2L_z^2}, \tag{8}$$

so that equation (6) becomes

$$\xi_z(t, x, z) = \sqrt{\frac{2}{\pi}} Z_0 L_x \sum_{n=0}^{\infty} \int_0^{+\infty} dk\, e^{-k^2 L_x^2/2} \times \cos(kx)\, \psi_n(z)\, \Psi_n\, \cos(\omega_n t), \tag{9}$$

where

$$\Psi_n = \int_{-\infty}^{+\infty} dz' \rho_{eq}(z') \psi_n(z') e^{-(z'-z_0)^2/2L_z^2}. \tag{10}$$

[22] Once the transversal displacement is computed, it is easy to obtain the other physical quantities such as the magnetic field or the thermal pressure through the following equations [*Fruit et al.*, 2002]:

$$P(\mathbf{r}) = P_{eq}(z - \xi_z)\left(1 - \gamma\left(\frac{\partial \xi_x}{\partial x} + \frac{\partial \xi_z}{\partial z}\right)\right), \tag{11a}$$

$$B_x(\mathbf{r}) = \left(1 - \frac{\partial \xi_z}{\partial z}\right) B_{eq}(z - \xi_z), \tag{11b}$$

$$B_z(\mathbf{r}) = \frac{\partial \xi_z}{\partial x} B_{eq}(z - \xi_z). \tag{11c}$$

[23] This theoretical model will now be used to interpret the Cluster data. For a precise and quantitative comparison it is worth to recall some numerical values. The characteristic half-width a of the Harris sheet is taken in accordance to the previous experimental analysis: $a = 0.2\ R_e \simeq 1280$ km. All the speeds are normalized to the speed of sound $v_s \simeq 800$ km/s. We thus deduce the timescale $\tau = a/v_s = 1.6$ s, which corresponds to a normalized frequency of 0.625 Hz.

3.2. Current Sheet Oscillations

[24] Before applying this theory, a last parameter must be specified: the ratio between the density in the central sheet and the density in the lobes. This parameter contributes to determine the shape of the dispersion curve and thus the coupling between the excitation and the eigenmodes. We choose it equal to 50, which means that the ratio between the Alfven speed in the lobes and the sound speed is about 7. These are reasonable values for the Earth magnetotail [*Lui*, 1987].

[25] The Figure 3 gives an example of signal reconstruction. As explained in paper 1 or in the work of *Fruit et al.* [2002], the eigenmodes are here obtained by solving equation (2) with boundary conditions corresponding to evanescent modes in the lobes. The colored isocontours of the thermal pressure (in nPa) are displayed versus time together with three black lines associated with a constant magnetic field; the central line is the neutral sheet. One gets a picture of the temporal evolution of the plasma sheet at a fixed x position, this coordinate being relative to the center of the initial excitation. We choose $x = 50a = 10\ R_e$. The comparison between this plot and the temporal reconstruction of the real plasma sheet observed by Cluster (Figure 2, panel 4) is thus straightforward. The geometrical parameters of the initial displacement are the following: $Z_0 = 4a \simeq 0.8\ R_e$, $L_x = 5a$, $L_z = a$, $z_0 = 5a$.

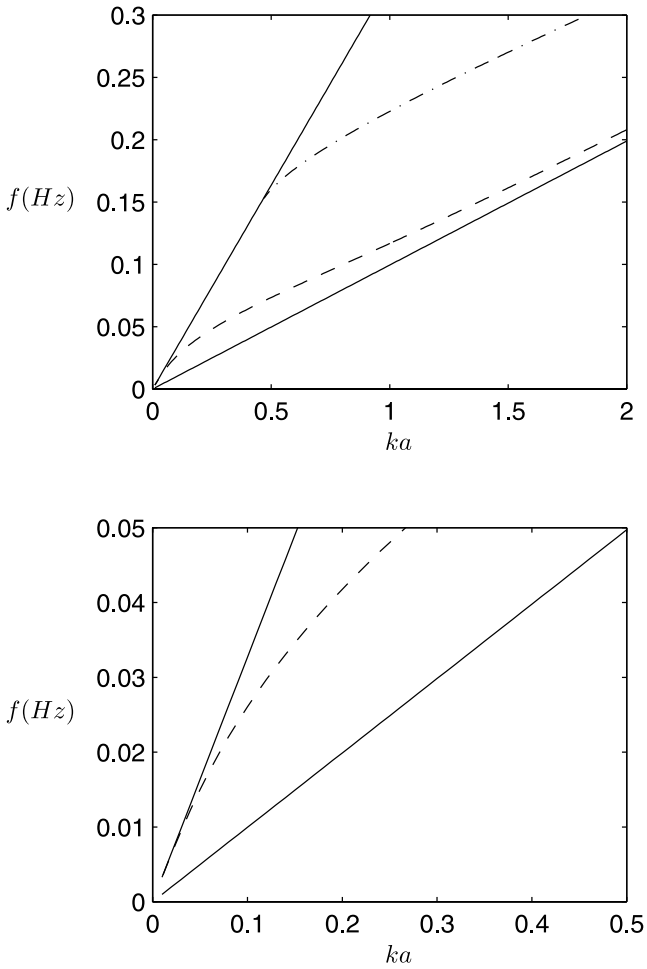

Figure 4. Dispersion relations in the current sheet. Dashed line: fundamental kink mode. Dotted-dashed line: first harmonic sausage mode. Solid lines: Alfven speed in the lobes and sound speed. The lower panel is a zoom of the upper one.

[26] The purpose of the analysis is not to exactly reproduce the sheet configuration observed from 0952 to 0954 (see Figure 2). The actual situation is indeed certainly more complex than the one considered theoretically. The point is rather to examine how the theoretical analysis may explain some general features of the observed oscillations. The first point to notice is that the model shows that both kink and sausage oscillations are excited. The initial displacement has indeed no symmetry properties, it thus excites as well the even kink mode as the odd sausage mode. For an initial centered displacement, only a kink oscillation would be generated. The kink fluctuations concern mainly the neutral sheet. They have a period of $\sim$20 s and an amplitude of about 0.15–0.2 R_e, which is in a very good agreement with the observations. The sausage oscillations affect the thickness of the sheet; they have period of the order of 6 s or a frequency of $\sim$0.16 Hz, which is also close to the second peak at 0.13–0.14 Hz observed in the experimental data. One also notices that the pressure fluctuations are dominated by the sausage mode. The corresponding dispersion diagram are displayed in Figure 4. The frequency is plotted directly in hertz by using the actual values of the normalization parameters. The lower graph is a zoom of the upper one for small wave numbers. We see that a frequency of 0.04 Hz corresponds to a wave number $ka = 0.2$ (wavelength of 6.3 R_e) for the fundamental mode (dashed line). This is consistent with the indirect estimate in section 2.2. The 0.16 Hz frequency is associated with the lower point of the first harmonic curve and the corresponding wavelength is about 2.5 R_e.

[27] The agreement between the observed frequencies and the ones predicted by the reconstruction procedure is remarkable. It was far from being obvious at the beginning that an initial excitation characterized by a broad spectrum with no distinct spectral peak could generate well-defined sinusoidal oscillations in the frequency ranges actually observed. Our results show that the Harris sheet behaves like a frequency filter, each mode being excited at specific frequencies. This point was already discussed by *Fruit et al.* [2002]. The interesting point here is that without a particular optimization, it is possible to reproduce the observed peaks from the theory. We check that reasonable modifications of the parameters of the initial displacement do not alter the spectral properties of the linear response of the sheet.

3.3. Global Magnetotail Oscillations

[28] The situation is however more intricate. Cluster indeed observes distinctly a sausage oscillation with a period of 20–25 s that is not predicted by the theoretical model developed above. The first harmonic sausage mode for a Harris sheet corresponds to a much higher frequency than the fundamental kink mode (see Figure 4) and it is impossible to generate both of them with the same period. The model of a simple Harris current sheet with modes that are evanescent in the lobes then does not explain all the characteristics of the observed sheet dynamics. We investigate another model that takes into account the global magnetotail (plasma sheet + lobes) and consider the magnetopause as boundary. The idea is that a more extended system in the z direction strongly reduces the eigenfrequencies, as does an electromagnetic waveguide, so that sausage modes at much lower frequencies than previously computed may exist.

[29] We consider that the thin current sheet, still modeled by an Harris profile with a typical width $a \simeq 0.2\ R_e$, is bordered by the two lobes. We still set to 50 the ratio between the density in the central sheet and the density in the lobes and assume a constant temperature (6 keV) in the sheet as well as in the lobes. Since the magnetopause is supposed to be a boundary of the system, we choose Dirichlet conditions of the type $\hat{\xi}_z = 0$ for $z = \pm l$, where l is the position of the magnetopause (we choose $l = 75a = 15\ R_e$). This choice is motivated by mathematical simplicity but also by physical grounds. We can indeed assume that the magnetopause constitutes a natural barrier for the waves that are guided within the global magnetotail.

[30] These boundary conditions change the nature of the eigenmodes. The dispersion diagram is recomputed and displayed on Figure 5. For high wave number, the dispersion curves still appear as lines parallel to the sound speed. They are almost identical to the dispersion curves obtained for free boundary conditions. When the wavelength is short, the eigenfunctions indeed appear as sharp peaks about $z = 0$ with a typical width of a few a. Thus the presence of the magnetopause is not noticeable in that case. On the contrary,

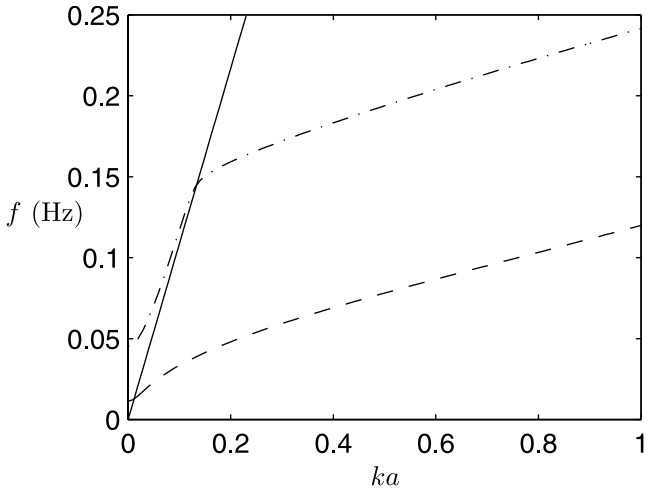

Figure 5. Dispersion relations in the global magnetotail. Same format as Figure 4.

when the wave number k tends to 0, the shape of the dispersion relations is significantly different from those previously shown. The frequency approaches a finite limit (cut-off frequency) with a vanishing group velocity. With the parameters chosen here, one verifies that the sausage mode can be excited with a frequency close to 0.05 Hz (corresponding to a period of 20 s). The MHD model might thus explain the low frequency sausage mode. It would nevertheless correspond to very small k values or to large wavelength (greater than 15 R_e). As already discussed in paper 1, it is hardly consistent with the Earth-Cluster distance.

[31] Having considered different possibilities in the framework of ideal MHD, we conclude that the low-frequency sausage mode, with wavelength of the order of 6 R_e (corresponding to approximately 30 times the sheet thickness), escapes the MHD description. We propose that it could be a tearing mode. It is interesting to note that it is observed as the sheet presents almost no B_z component, a situation known to favor tearing modes. More works are needed to firmly establish this interpretation.

3.4. Relative Amplitudes of the Magnetic and Pressure Fluctuations

[32] We now go further in the analysis and investigate the relative amplitudes and phasing of the magnetic and pressure fluctuations. We consider here the sausage oscillations since they lead to much larger pressure variations than the kink mode.

[33] This analysis is presented in Figure 6. On the two upper panels, we plot the sheet configuration retaining the sausage mode only (symmetric variations of a). A color code indicates the averaged pressure measured by SC1, SC3, and SC4. On panel 1 we consider the total pressure (magnetic + thermal) variations. Assuming that the sheet dynamics obeys to a condition of pressure balance with the

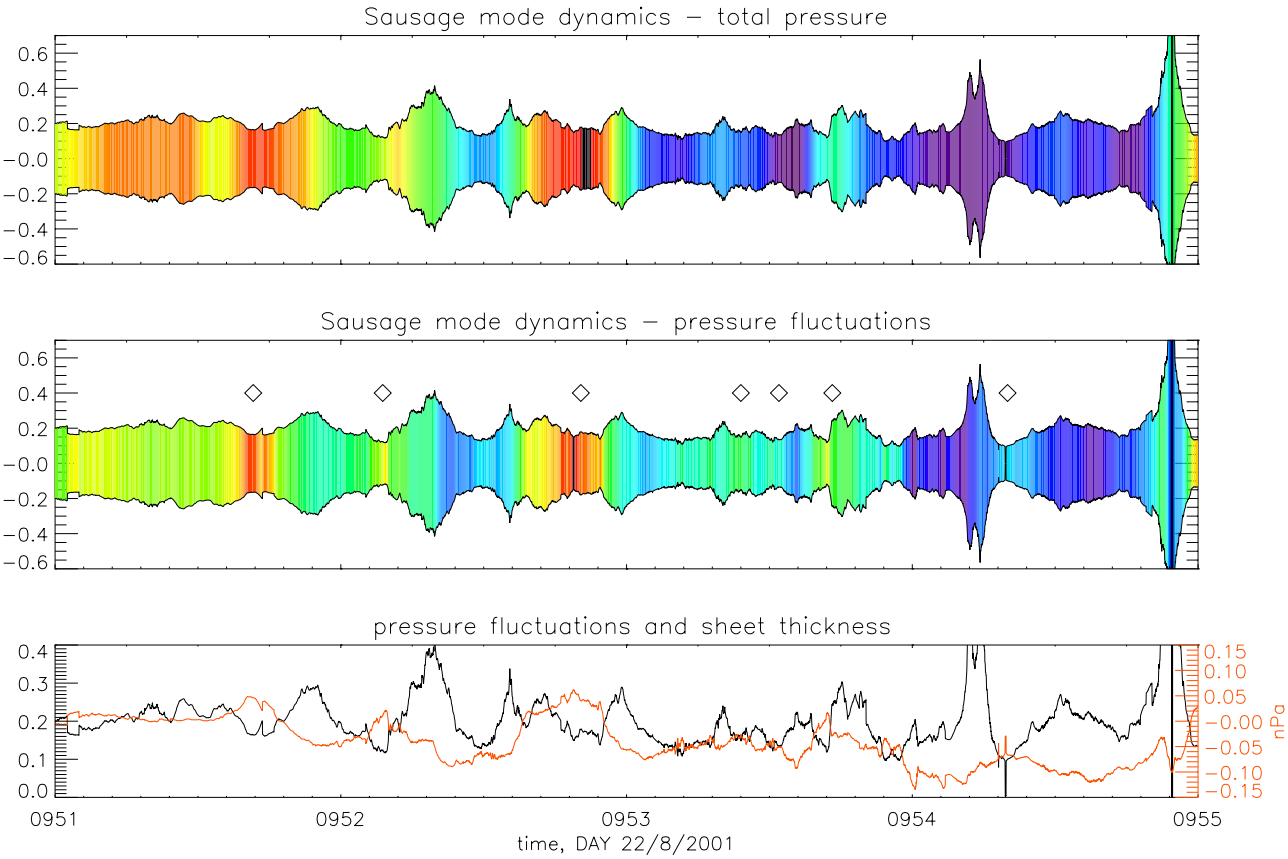

Figure 6. Analysis of the dynamics of the sausage mode. From top to bottom, Panel 1: thickness variations and total pressure fluctuations; Panel 2 and 3: thickness variations and compressibility contributions of the pressure fluctuations.

lobes, it is then possible to verify if the variations of the sheet thickness is directly linked to external pressure fluctuations. This does not seem to be the case, since such a systematic behavior is not observed. The thinnings of the sheet are almost randomly associated to total pressure increases or decreases. We thus conclude that the variations of the sheet thickness are not simple one-to-one consequences of external pressure fluctuations. This suggests that the oscillations are most probably the result of the intrinsic dynamics of the sheet.

[34] On panel 2, we plot the intrinsic thermal pressure fluctuations of the sheet. The pressure fluctuations measured by the spacecraft are indeed the sum of two terms (see equation (11a)): (1) a fluctuation due to the vertical motion of the sheet (convective term): $P_{eq}(z - \xi_z)$ and (2) an intrinsic fluctuation due to the compressibility of the plasma (compressibility term): $-\gamma P_{eq}(\partial\xi_x/\partial x + \partial\xi_z/\partial z)$. We consider this second term in Figure 6, since it is the most meaningful for the sausage-mode dynamics. In the theoretical model it is straightforward to distinguish the two terms. Here, the convective terms can be estimated by considering the pressure of a nonperturbed Harris sheet that has been displaced accordingly to the results of the Harris fit. The compressibility term is then estimated by computing the difference between the thermal pressure actually measured by the spacecraft $P_{SC}(t)$, and this convective term $P_{eq}(\xi_z(t))$ where $\xi_z(t)$ is the measured vertical displacement and P_{eq} is the Harris pressure profile. If the dynamics of the sheet is dominated by a MHD sausage eigenmode, one expects pressure increases as the sheet thins. This is actually observed. At the exception of the noticeable thinning occurring at ~0952:30, thinning of the sheet and intrinsic pressure increases are indeed correlated. This is particularly well observed from 0953 to 0954 as the higher-frequency sausage mode (0.14 Hz) dominates. Diamond symbols indicate some of these correlations.

[35] It is also possible to verify that the observed relative amplitudes of the magnetic and pressure fluctuations are consistent with the theoretical predictions. The observed fluctuations are plotted in panel 3. From this plot, one can consider that thickness variations of 0.1 R_e correspond to pressure variations of the order of 0.1 nPa. This is slightly less than what is predicted by the theoretical model. As seen in Figure 3, a variation of 0.1 R_e corresponds to approximately 0.15 nPa.

4. Conclusion

[36] One lesson of our investigation is thus the remarkable agreement obtained between the observation of some types of plasma sheet oscillations and the complete theory of the MHD response of a Harris sheet to external excitations. Nevertheless, this is certainly not a generality. In paper 1 we show that the fluctuations observed by Cluster with periods larger than typically 100 s are very unlikely freely propagating MHD eigenmodes. Given the physical and geometrical properties of the sheet deduced from Cluster measurements, these fluctuations would indeed have wavelength larger than the Earth/Cluster distance or the Y extension of the magnetotail. This type of fluctuations is dominant during the quiet magnetospheric period and would correspond to fluctuations that slowly propagate in the Y direction, with a typical velocity of a few 10 km/s. Their physical nature remains to be determined.

[37] However, following a substorm onset, fluctuations with periods of the order of 20–25 s are also detected. They appear to be compatible with the theoretical predictions concerning the MHD dispersion properties of a Harris sheet. In the present paper, by investigating the linear MHD response of a Harris sheet to an external perturbation and performing the full signal reconstruction, we show that the spectral characteristics of the fluctuations can be interpreted as a natural frequency selection of the sheet. The observed kink-like and sausage-like oscillations (at 0.04 Hz and 0.14 Hz) both propagating in the x direction have indeed frequencies very close to the theoretical spectral peaks. The amplitudes of the oscillations are also compatible with excitations of reasonable level: an initial vertical displacement of the sheet with an amplitude and a gaussian x extension of a few times the sheet thickness (4 and 5 times, respectively). Displacements of such amplitudes are actually observed with Cluster during the sheet crossing considered here. As shown here, the linear MHD response theory demonstrates that such excitations trigger oscillations with global characteristics (frequency spectra, amplitudes, spatial organization in restricted wave packets) very close to the observed ones.

[38] We also identify a low-frequency sausage mode at 0.04 Hz that is not easily explained by the MHD model. We show that an ideal MHD interpretation is not formally impossible if eigenmodes coupled to the magnetopause thus including the plasma sheet and the lobes are considered. They would nevertheless have very large wavelength compared to the Earth/Cluster distance. We thus conclude that the existence of this sausage mode, in exact phasing with the kink-like MHD oscillation, remains to be understood. It could correspond to a tearing mode and this interesting possibility will be investigated in the future.

[39] **Acknowledgments.** Lou-Chuang Lee thanks Rudolf A. Treumann and another reviewer for their assistance in evaluating this paper.

References

Cornilleau-Wehrlin, N., et al. (1997), The Cluster Spatio-Temporal Analysis of Field Fluctuations (STAFF) experiment, *Space Sci. Rev.*, *79*, 107–136.

Fruit, G., P. Louarn, A. Tur, and D. Le Quéau (2002), On the propagation of magnetohydrodynamic perturbations in a Harris-type current sheet: 1. Propagation on discrete modes and signal reconstruction, *J. Geophys. Res.*, *107*(A11), 1411, doi:10.1029/2001JA009212.

Louarn, P., G. Fruit, E. Budnik, C. Jacquey, D. Le Quéau, H. Rème, E. Lucek, and A. Balogh (2004), On the propagation of low-frequency fluctuations in the plasma sheet: 1. Cluster observations and magnetohydrodynamic analysis, *J. Geophys. Res.*, *109*, A03216, doi:10.1029/2003JA010228.

Lui, A. T. (1987), *Magnetotail Physics*, Johns Hopkins Univ. Press, Baltimore, Md.

Nakamura, R., et al. (2002), Fast flow during current sheet thinning, *Geophys. Res. Lett.*, *29*(23), 2140, doi:10.1029/2002GL016200.

A. Balogh and E. Lucek, Imperial College, South Kensington Campus, London SW7 2BZ, UK. (a.balogh@ic.ac.uk; e.lucek@ic.ac.uk)

E. Budnik, C. Jacquey, D. Le Quéau, P. Louarn, H. Rème, and J. A. Sauvaud, Centre d'Etude Spatiale des Rayonnements, 9 avenue du Colonel Roche, BP 4346, 31028 Toulouse cedex 4, France. (budnik@cesr.fr; jacquey@cesr.fr; lequeau@cesr.fr; louarn@cesr.fr; reme@cesr.fr; sauvaud@cesr.fr)

N. Cornilleau-Wehrlin, Centre d'Etudes Terrestres et Planétaires, Vélizy, France. (nicole.cornilleau@cetp.ipsl.fr)

G. Fruit, University of Waikato, Private Bag 3105, Hamilton, New Zealand. (fruit@math.waikato.ac.nz)